Distributed feedback laser for biosensing applications

A-M Haughey*, B Guilhabert*, M D Dawson*, G A Burley†, and N Laurand*
*Institute of Photonics, SUPA, University of Strathclyde, Glasgow G4 0NW, UK
†WestCHEM, Department of Pure and Applied Chemistry, University of Strathclyde, Glasgow G1 1XL, UK
Email: annemarie.haughey@strath.ac.uk

***Abstract*—We present an organic semiconductor distributed feedback laser biosensor and demonstrate its sensing capabilities. Optimization of the gain layer thickness to maximize the response to refractive index changes and bulk sensing results are shown. Desthiobiotin-avidin sensing assay results are also presented and the potential to perform multiple, repeated sensing measurements is demonstrated.**

I. Introduction

Evanescent optical sensors are devices that measure a change in the refractive index of the medium at the sensor surface. Such sensors are ideal for medical diagnostic applications due to their capacity for non-contact label-free detection, multiplexing and their incorporation into lab-on-chip systems [1]–[4]. Distributed feedback (DFB) lasers represent one type of evanescent biosensor that can be used to observe refractive index changes in liquid or gaseous media, via a change in emission wavelength as shown in Fig.1. DFB lasers are simple in their fabrication and can be excited optically at any position within the sensor surface and generate their own coherent, narrow stimulated emission normal to the laser surface, resulting in simple implementation [5], [6]. The surface of a DFB laser can be functionalized for the detection of specific analytes; binding of the target analytes produces a change in refractive index at the laser surface which translates to a corresponding change in emission wavelength that is detected. Existing DFB laser biosensors utilize a dye-doped polymer as the gain material and have been shown to detect a variety of different biomolecules [7], [8]. Here, we discuss an 'all-organic' oligofluorene truxene-based DFB laser biosensor. By using an organic semiconductor as the gain material, which is less prone to quenching than dye-doped polymers, there is potential to enhance laser, and therefore sensing, characteristics.

DFB laser sensitivity for refractive index sensing is defined by the material and structural properties of the device [9], [10]. Therefore, it is important to understand the influence each of the device parameters have on the operation and response of the laser to refractive index changes. The effect of device parameters on refractive index sensing can be investigated through the use of an analytical model. Modeling of the device response to bulk or surface sensing (i.e. biomolecule detection) can be an efficient way to determine the optimum DFB laser structure design to maximize device sensitivity.

In this paper we present a modified slab waveguide model used to characterise the response of our DFB lasers and optimize the structure for surface sensing. We also present specific biomolecule (avidin) detection results and demonstrate that a single sensor can be used for repeated avidin detection measurements. The "plastic" nature of our DFB lasers make them suitable for single-use disposable sensors, nonetheless, the prospect of a robust multi-use sensor is an attractive concept.

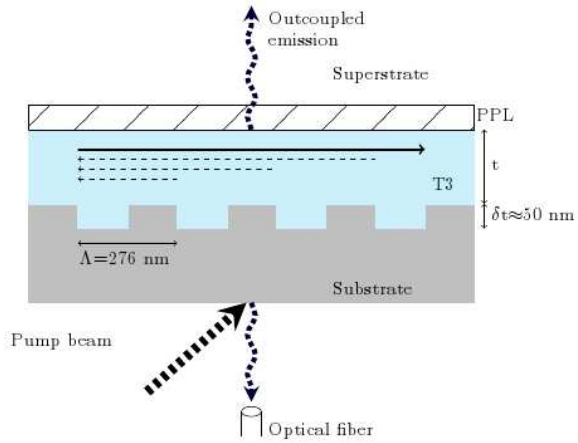

(a)

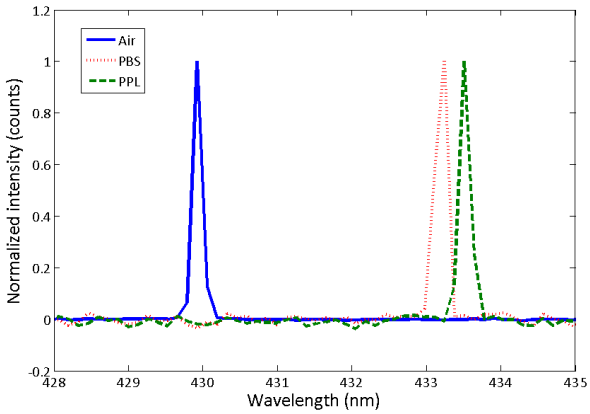

(b)

Figure 1. Schematic of the DFB laser with a monolayer of polyphenylalanine lysine (PPL) deposited on the truxene (T3) surface. Laser emission is normal to the device surface and is coupled to a spectrometer. The solid and dashed lines represent the propagation of the second order laser mode and the feedback induced by perturbations in refractive index due to the grating structure respectively (a). Examples of spectral emission with the laser superstrate as air, phosphate buffered saline (PBS) solution and 1 mg/mL PPL in PBS solution (b).

II. Device concept

The sensor is based on a second-order vertically-emitting DFB laser and consists of a three-layer planar

978-1-4244-7929-0/14/$26.00 ©2014 IEEE

waveguide with a thin gain layer, thickness t=70 nm, sandwiched between the substrate and superstrate regions as shown in Fig.1a. The substrate, a UV curable optical epoxy (Norland), is patterned with a periodic nanostructure (period, Λ, 276 nm; grating depth, δt, 50 nm) which provides both the out-coupling and feedback mechanism for the laser. The gain layer is an organic semiconductor composed of fluorescent tris(terfluorenyl)truxene (T3). T3 has a refractive index of 1.81 at 430 nm in a thin film [11] which is higher than the refractive indices of the substrate and superstrate, i.e. forming a planar waveguide.

$$\lambda = n_{eff}\Lambda \tag{1}$$

DFB laser emission is governed by the second-order Bragg equation, Equ. 1, where λ is the Bragg wavelength, n_{eff} is the effective refractive index of the mode, and Λ is the grating period as defined previously. The value of n_{eff} is determined by the refractive indices of each of the three layers and the thickness of the T3 layer. Any change in the superstrate refractive index, such as a change in superstrate medium or adsorption of molecules to the laser surface, will influence the effective refractive index and induce a shift in the laser emission wavelength, as demonstrated in Fig. 1b. Therefore, the DFB laser can be used for biosensing applications via functionalization of the laser surface for specific biomolecule detection and monitoring the emission wavelength of the laser.

A. Simulation of laser response

Simulation of the effective refractive indices of the laser modes, and the shifts in laser emission wavelength, was performed using a modified one-layer waveguide model of the DFB laser [12], [13]. The model inputs are the structure parameters such as refractive index and thickness, and the model outputs the effective refractive index for the structure. The effect of the periodic modulation induced by the grating structure and the effect of refractive index dispersions of both the substrate material and the T3 were taken into account in the model as has been described previously elsewhere [14]. For simulation of surface sensing, the model was modified to consider multiple layers enclosed between semi-infinite substrate and superstrate regions [15]. Examples of the modeled response of the DFB laser to changing superstrate index (air, PBS solution and PPL solution) are shown in Fig. 2, demonstrating the change in the electric field for changing effective refractive index.

B. Device fabrication

DFB lasers were fabricated by drop-coating an optical epoxy onto a silica master grating (E-beam lithography), with a piece of acetate sheet on top, and photocuring with a UV lamp for 50 s. After curing, the grating imprinted epoxy was peeled from the master grating and cured for a further 60 minutes. T3 solution (20 mg/mL) was prepared in toluene and 20 μL spin-coated onto the grating imprinted epoxy at a range of spinning speeds for 90 s (see Section IIIA). Sensors were fixed within a

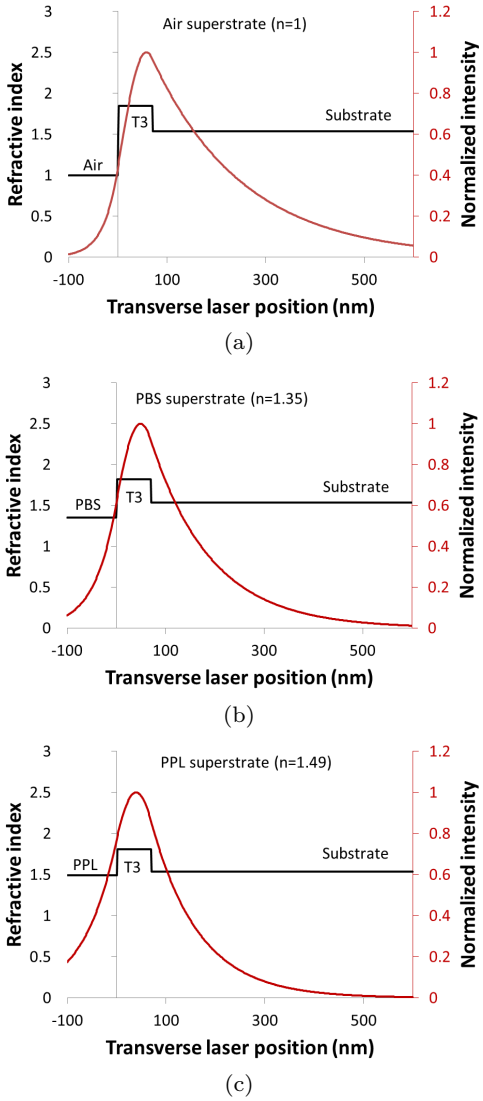

Figure 2. Modeled electric field profiles for the laser exposed to air (a), PBS solution (b) and PPL solution (c).

glass cuvette and were pumped through the substrate, at an external angle of $\approx 45^o$, with a frequency-tripled, Q switched Nd:YAG laser (355 nm, 10 Hz repetition rate) and out-coupled emission was collected by an optical fiber and transferred to a grating-coupled CCD spectrometer. The laser can be pumped at any position within the greating and an angle of 45^o was simply chosen for the ease of collecting emission normal to the laser surface.

III. Results

A. Gain layer optimization

The thickness of the T3 layer is directly related to the laser mode wavelength and the sensitivity of the DFB laser response to bulk refractive index changes. A minimum T3 thickness is required for lasing but beyond this minimum cut-off thickness, a thinner gain layer results in a greater shift in wavelength emission per refractive index unit (RIU) change. The response of our DFB laser was investigated by preparing a number of lasers with a

range, 0.5 - 3.5 thousand revolutions per minute (krpm), of different T3 spin-coating speeds. The response of these lasers to bulk refractive index changes was probed by submerging the lasers in de-ionised (DI) water (refractive index of approximately 1.34 at 430 nm). The laser wavelengths (in air) and the shifts in emission wavelength upon exposure to DI water for each of the lasers are shown in Fig. 3. The largest shifts in wavelength ($\Delta\lambda\approx3.40$ nm) were noted for lasers with the lowest lasing wavelength i.e. lasers with the T3 layer spin-coated at the fastest speeds and therefore with the thinnest gain layers. The expected shift in wavelength upon exposure to DI water was also modeled as a function of gain layer thickness as shown in Fig. 3. The theoretical data agrees well with the experimental data, a plateau at a maximum wavelength shift of ($\Delta\lambda$=3.31 nm) for a gain layer thickness between 65-75 nm. The T3 layer thickness was determined using atomic force microscopy and demonstrated that a spin-coating speed of 3.2 krpm resulted in a T3 thickness of 70.6±9.0 nm, within the plateau region of the modeled shift. The mean shift in wavelength for lasers spin-coated at 3.2 krpm was 3.33±0.07 nm upon exposure to DI water. Therefore, all lasers were subsequently fabricated with a spin-coating speed of 3.2 krpm. The good agreement between the experimental and theoretical results indicates that the model can be used to investigate design changes to the DFB laser structures for sensitivity optimization with confidence.

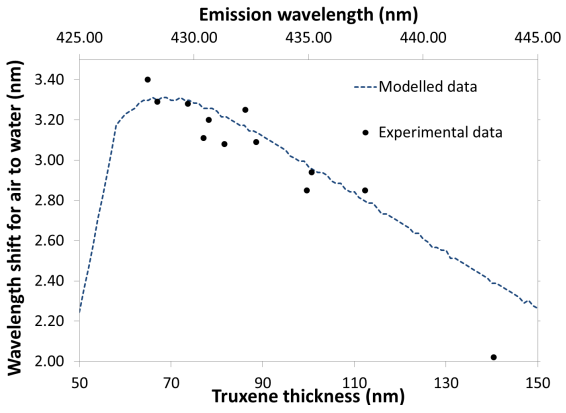

Figure 3. The shift in wavelength and emission wavelength in air for lasers fabricated with a range of T3 thicknesses are plotted. Theoretical thickness, emission wavelength and wavelength shifts are also plotted.

B. Bulk sensitivity

Bulk refractive index sensing was demonstrated by immersing DFB lasers in solutions with a range of different refractive indices as shown in Fig. 4. The laser emission was found to redshift >5 nm for the 60% glycerol solution which was the highest index solution tested. This corresponds to a bulk refractive index sensitivity ($\Delta n/\Delta\lambda$) of 23 nm/RIU. The shift in wavelength for increasing bulk refractive index was also determined for the DFB laser for a range of superstrate refractive indices using the model, also shown in Fig. 4. The model over estimates the wavelength shift for changing refractive index slightly. This may be in part be due to the estimates of the refractive indices of our test solutions at 430 nm. Whilst the bulk refractive index sensitivity is currently lower than the sensitivities reported for optimised dye-doped DFB lasers (≈100 nm/RIU), the improvement in sensitivity for these lasers can be attributed to two points: i, dye-doped lasers tend to operate at longer wavelengths and have a longer Λ value which results in a greater shift in wavelength for bulk sensing and ii, the addition of a high-index TiO_2 cladding layer deposited on top of the gain layer during fabrication [5]. Our multi-layer model suggests that a significant improvement in bulk sensitivity would be attained if a thin, high-index TiO_2 cladding layer was deposited onto the T3 surface and the addition of TiO_2 cladding layer to our lasers is currently being investigated. Bulk detection sensitivity is a useful metric for comparing waveguide based refractive index sensors. However, as this sensor is intended for specific biomolecule detection, the response of the sensor to interactions at the surface provides a more appropriate measure of the sensor performance for biosensing applications.

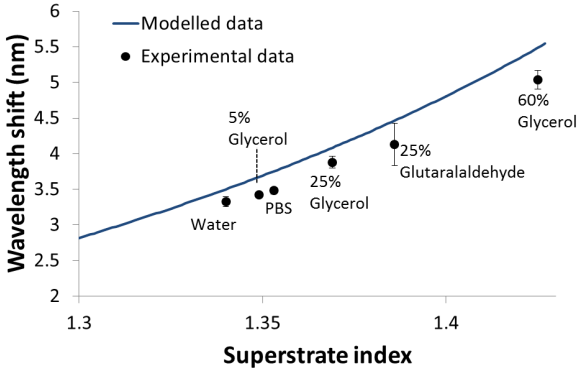

Figure 4. Bulk refractive index measurements are plotted alongside the theoretical wavelength shift for increasing superstrate index.

C. Reversible biomolecule detection

In order to investigate the capability of our DFB laser for specific biomolecule detection, a desthiobiotin-avidin assay was performed. Desthiobiotin is a biotin analogue with a lower binding affinity for avidin (dissociation constant (K_d)≈10^{-11} M) relative to that of biotin ($K_d\approx10^{-15}$ M). Fig. 5 presents our results demonstrating specific detection of avidin on a desthiobiotin functionalized laser. Sensor functionalization was achieved by immersion of the sensor in PPL (1 mg/mL) prepared in 10 mM PBS for 10 minutes before rinsing with PBS and a further submersion of the laser in NHS-LC-desthiobiotin (0.2 mg/mL) in 10 mM PBS for 20 minutes. After rinsing with PBS, the sensor was immersed in avidin solution for 20 minutes. Avidin detection at a range of concentrations is shown in Fig. 5a. Saturation of the desthiobiotin binding sites occured at an avidin concentration of around 0.1 mg/mL. A different DFB laser sensor was used for

each of the avidin concentrations. The minimum "detectable" shift in wavelength is defined as a shift with a magnitude of three times the standard deviation [16]. The standard deviation of the wavelength shift for multiple avidin binding measurements was measured to be 0.02 nm. Therefore, limit of avidin detection was ≈2.5 μg/mL.

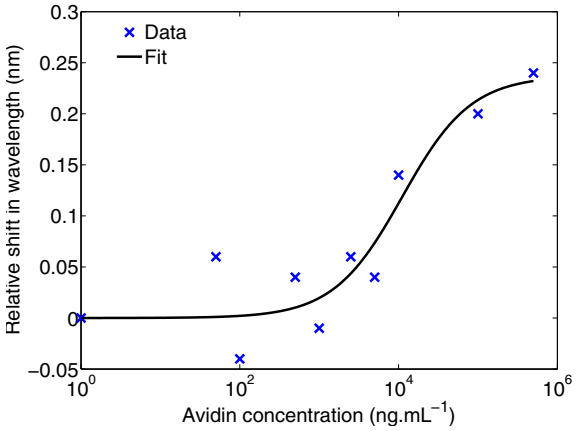

(a)

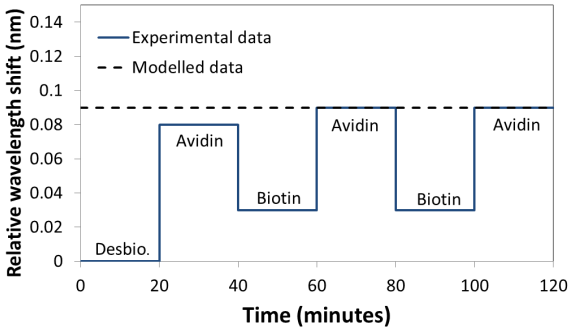

(b)

Figure 5. Avidin detection results for a desthiobiotin functionalized laser (a). The shift in emission wavelength relative to a baseline PBS wavelength are shown for a PPL and desthiobiotin functionalized sensor and exposed to repeated avidin and biotin solutions. The dashed line represents the predicted shift in wavelength for an avidin monolayer (b).

Due to the stronger binding affinity, binding between biotin and avidin is inherently more efficient than that of desthiobiotin and avidin (avidin limit of detection ≈1 μg/mL) [17]. However, the use of desthiobiotin allows bound avidin to be released from desthiobiotin simply by treating the laser with a biotin solution (0.2 mg/mL), resulting in a "re-usable" sensor. The shift in wavelength for the functionalization of the laser with PPL and desthiobiotin and subsequent avidin binding and removal is shown in Fig. 5b. The relative shifts in wavelength after each exposure to avidin solution (10 μg/mL) correspond to the relative shifts in wavelength after exposure to biotin, indicating that most of the avidin bound to the desthiobiotin functionalized sensor was released after treatment of the laser with biotin solution and that repeated and reproducible avidin binding was possible. The shift in wavelength for a desthiobiotin functionalized sensor exposed to avidin was modeled using the multilayer model. The dimensions of avidin are ≈4x4x6 nm [18] therefore a layer thickness of 4 nm was assumed for a confluent avidin layer, with a refractive index of 1.4. Using these parameters, the model predicts a shift in wavelength emission of 0.09 nm for an avidin monolayer, shown in Fig. 5b, which corresponds to the experimental shifts measured.

IV. Conclusion

Optimization of the gain layer thickness is demonstrated using both experimental measurements and theoretical results from a modified waveguide model. Both the bulk and surface sensing capabilities of a truxene-based plastic DFB laser are also demonstrated. The wavelength shifts upon exposure to a selection of solutions with a range of refractive indices were measured and shown to correlate well with theoretical results from the model. The potential of our laser as a re-usable biosensor was demonstrated via a desthiobiotin-avidin bioassay. Future development of our DFB laser will focus on improvement of both the bulk and surface sensitivity in order to facilitate the detection of other biomolecules such as nucleic acids and proteins.

Acknowledgment

This work was supported by EPSRC grants EP/J021962/1 and EP/I029141/1.

References

[1] M. Kristensen *et al.*, in *Optical Sensors*, 2011, p. SWB1.
[2] V. Koubová *et al.*, *Sensors and Actuators B: Chemical*, vol. 74, pp. 100 – 105, 2001.
[3] M. Baaske *et al.*, *ChemPhysChem*, vol. 13, pp. 427–436, 2012.
[4] B. Cunningham *et al.*, *Sensors and Actuators B: Chemical*, vol. 87, pp. 365 – 370, 2002.
[5] Y. Tan *et al.*, vol. 12, pp. 1174 –1180, may 2012.
[6] Y. Yang *et al.*, *Applied Physics Letters*, vol. 92, p. 163306, 2008. [Online]. Available: http://link.aip.org/link/?APL/92/163306/1
[7] M. Lu *et al.*, *Applied Physics Letters*, vol. 92, p. 261502, 2008.
[8] M. Lu *et al.*, *Applied Physics Letters*, vol. 93, pp. 111 113 –111 113–3, sep 2008.
[9] I. D. Block *et al.*, *Sensors Journal, IEEE*, vol. 8, pp. 274–280, March 2008.
[10] C. Vannahme *et al.*, *Laser and Photonics Reviews*, vol. 7, pp. 1036–1042, 2013. [Online]. Available: http://dx.doi.org/10.1002/lpor.201300083
[11] G. Tsiminis *et al.*, *Applied Physics Letters*, 2009.
[12] P. K. Tien, *Appl. Opt.*, vol. 10, pp. 2395–2413, Nov 1971. [Online]. Available: http://ao.osa.org/abstract.cfm?URI=ao-10-11-2395
[13] H. Kogelnik, *Microwave Theory and Techniques, IEEE Transactions on*, vol. 23, pp. 2–16, 1975.
[14] A. Haughey *et al.*, *Sensors and Actuators B: Chemical*, vol. 185, pp. 132–139, 2013.
[15] J. Chilwell *et al.*, *J. Opt. Soc. Am. A*, vol. 1, pp. 742–753, Jul 1984. [Online]. Available: http://josaa.osa.org/abstract.cfm?URI=josaa-1-7-742
[16] B. Cunningham, M. Cooper, Ed. Cambridge University Press, 2009, pp. 1–28.
[17] A. Haughey *et al.*, *Biosensors and Bioelectronics*, vol. 54, pp. 679–686, 2014.
[18] N. M. Green *et al.*, *Biochemical Journal*, vol. 118, p. 681.b1, 1970.